Ribbon phase in a phase-separated lyotropic lamellar-sponge mixture under shear flow

G. Cristobal,[1] J. Rouch,[1] P. Panizza,[1,*] and T. Narayanan[2]
[1]*Centre de Physique Moléculaire Optique et Hertzienne, Université Bordeaux I, 351 Cours de la Libération, 33400 Talence, France*
[2]*European Synchrotron Radiation Facility, 38043 Grenoble, France*
(Received 8 February 2001; published 22 June 2001)

We report the effect of shear flow on a phase-separated system composed of lyotropic lamellar (L_α) and sponge (L_3) phases in a mixture of brine, surfactant, and cosurfactant. Optical microscopy, small-angle light, and x-ray scattering measurements are consistent with the existence of a steady state made of multilamellar ribbonlike structures aligned in the flow direction. At high shear rates, these ribbonlike structures become unstable and break up into monodisperse droplets resulting in a shear-thickening transition.

DOI: 10.1103/PhysRevE.64.011505 PACS number(s): 68.05.Gh, 47.20.Hw, 64.75.+g

I. INTRODUCTION

Dispersing one fluid into another immiscible one is an everyday experience (e.g., mixing milk with coffee, preparing salad sauces, etc.) that requires the use of shear flow to rupture large drops into small droplets [1–4]. Since the pioneering work of Taylor on dilute emulsions [5], many authors have studied the interplay between surface tension, viscosity, and flow that leads to the deformation and breakup of droplets under shear flow. In the past, extensive works along this line have been carried out on partially miscible binary mixtures undergoing phase separation, e.g., semidilute polymer solutions, near-critical and off-critical liquid mixtures, etc. [6–9]. When the viscosities of both phases are similar, the dispersed phase forms somewhat deformed droplets of the order of the breakup size $R_b \approx \sigma/(\eta\dot{\gamma})$, where σ is the surface tension, η is the viscosity, and $\dot{\gamma}$ is the shear rate. Light scattering experiments in off-critical binary mixtures [8] and polymer solutions [9] have revealed nearly monodisperse distributions of droplets of the minority phase with size of the order of R_b, which scales like the inverse of the shear rate. When both phases are percolated (as in near-critical mixtures), the competition between flow and coarsening results in a very different steady state known as the ''string phase'' [10], consisting of strikingly elongated cylindrical domains along the flow direction. The existence of such a string phase is quite surprising since a long cylinder of fluid at rest would normally break up via the Rayleigh instability. However, Frischknecht [11] has recently shown that the shear flow can stabilize both the hydrodynamic Rayleigh instability and the thermodynamic instability of a cylinder against various perturbations by mixing with nonaxial symmetric perturbations.

In this article, we report the effect of shear flow on a phase-separated lamellar-sponge fluid composed of brine, surfactant, and cosurfactant. Contrary to other systems studied before, here one of the coexisting phases possesses bending elasticity that adds up to the interplay among surface tension, viscosity, and flow and can modify the microstructure in the steady states. In this system, we observed the existence of a new steady state consisting of ribbonlike structures, aligned in the flow velocity direction. At high shear rates, these ribbons become unstable and fragment into monodisperse droplets corresponding to a shear-thickening transition.

II. EXPERIMENTAL METHODS

The experimental system consisted of a quaternary mixture of sodium dodecyl sulfate (SDS), octanol, and brine (20 g/l of NaCl). The phase diagram of this system exhibits a coexisting region between lamellar (L_α) and sponge (L_3) phases at room temperature [12]. While the membranes are stacked with smectic order in the (L_α) phase, the sponge phase is made of disordered and multiply connected membranes that divide the solvent into two equivalent subvolumes [13]. In addition, their rheological behavior is drastically different; L_3 phase is usually a low viscous Newtonian fluid whereas L_α phase presents strong non-Newtonian behavior as a result of the strong coupling between the microstructure and the flow field [14,15]. It should be noted that in some systems shear flow induces a sponge-to-lamellar phase transition [16,17]. However, the small-angle x-ray scattering (SAXS) data described below clearly exclude this possibility in our system.

We have worked with a sample composed of 11.35% of SDS (Prolabo), 13.65% of octanol, and 75% of water containing 20 g/l of NaCl by weight. This solution is a lamellar phase below 30 °C and a sponge phase above 40 °C. At intermediate temperatures, the mixture separates into coexisting L_α/L_3 phases, with the macroscopic meniscus appearing within a few minutes when left unstirred. Small shifts in the transition temperatures can be observed from sample to sample due to the composition and purity of the chemical used. In order to study the effect of shear flow on the L_α/L_3 mixture, we first allowed the solution to reach equilibrium in the one-phase region below 30 °C and then performed a temperature quench of the sheared solution to bring it to the L_α/L_3 coexistence region. After a few minutes, a macroscopically homogeneous steady state is reached, provided the shear rate is $>10\ s^{-1}$ to prevent macroscopic demixing [18]. We have studied the structure of these steady states as a function of shear rate over the temperature range 30–40 °C. The results presented below pertain to 33 °C that corresponds

*Author to whom correspondence should be addressed: Email address: ppanizza@cribxl.u-bordeaux.fr

 ©2001 The American Physical Society

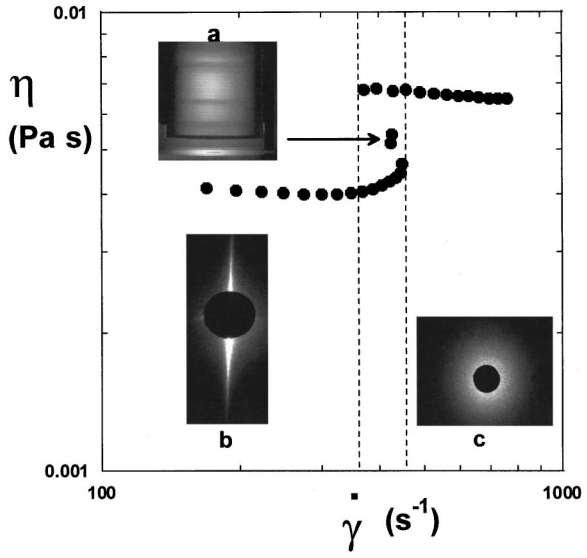

FIG. 1. Viscosity as a function of shear rate at 33 °C. Inset a: flow visualization in the Couette cell in the reentrant region corresponding to an imposed stress of 2 Pa. The velocity $\vec{V}$ and vorticity $\vec{Z}$ directions are horizontal and vertical, respectively. SALS pattern in the $(\vec{q}_v,\vec{q}_z)$ plane at 33 °C for $\dot{\gamma}<370\,\mathrm{s}^{-1}$ (inset b) and $\dot{\gamma}\geqslant 480\,\mathrm{s}^{-1}$ (inset c).

to a lamellar phase volume fraction of 45% in the mixture.

The rheological characterization of these steady states was performed with a Rheometrics RS5 rheometer, which was operated under constant stress mode. The transparent Couette cell consisted of a stator and a rotor with diameters 19 and 20.5 mm, respectively. The experimental setup used to measure the small-angle light scattering (SALS) under shear flow (shear rate imposed) in the velocity-vorticity $(\vec{V},\vec{Z})$ plane has been described elsewhere [18]. The SAXS measurements of sheared samples were performed on the ID-2 beamline at the ESRF in Grenoble, France. The wavelength λ of the incident monochromatic radiation was 0.1 nm and the beam size was $100\times 300\,\mu\mathrm{m}^2$ (horizontal and vertical directions, respectively). The scattered intensities were recorded by an image intensified charge-coupled device detector with an active area of size about 230 mm and pixel size 0.175 mm. The polycarbonate Couette cell consisted of a stator and a rotor whose diameters are 10 and 12 mm, respectively. The data reported here correspond to a distance between sample and detector of 5 m. The sample temperature was controlled to within 0.01 °C and the shear rate was varied between 10 and 1000 s^{-1}. By translating the cell across the beam, we recorded the SAXS pattern in the $(\vec{V},\vec{Z})$ (radial beam configuration) and $(\nabla\vec{V},\vec{Z})$ (tangential beam configuration) planes, where $\vec{V}$, $\vec{Z}$, and $\nabla\vec{V}$ refer to directions of the flow velocity, the vorticity, and the velocity gradient, respectively.

III. RESULTS

Figure 1 shows the behavior of viscosity η as a function of shear rate $\dot{\gamma}$. It displays two branches corresponding to low and high shear rates (or stresses), where the mixture is Newtonian. These two branches are separated by a reentrant region, in which η is a decreasing function of $\dot{\gamma}$. In this region, when the stress is fixed, the flow visualization indicated the existence of shear bands (see inset a in Fig. 1). These shear bands reveal a coexistence between two steady states found at low and high shear rates (or stresses) [19–21]. According to Olmsted's classification [21], the observed pattern (horizontal bands in the Couette cell, see inset a in Fig. 1) is characteristic of a ''$B2$ common strain rate phase separation'' when the stress is fixed. We investigated the structure of the two steady states found at low and high stress (i.e., shear rates) by means of small-angle light scattering, optical microscopy, and small-angle x-ray scattering. At low shear rates (i.e., $\dot{\gamma}\leqslant 370\,\mathrm{s}^{-1}$), in small-angle light scattering we observed a streak pattern elongated along the vorticity direction as shown in Fig. 1 (inset b). It is worth noting that this pattern is identical whether or not the stress is fixed instead of the shear rate. A similar scattering pattern has already been observed by Hashimoto and co-workers in the case of the ''string phase'' [10]. This streak pattern directly indicates the presence of some very anisotropic structures aligned in the flow velocity direction. This strong anisotropy disappears within a few seconds up on the cessation of shear. The texture observed at rest under a polarizing microscope showed the presence of very large lamellar droplets still slightly elongated along $\vec{V}$ and immersed in the L_3 matrix as

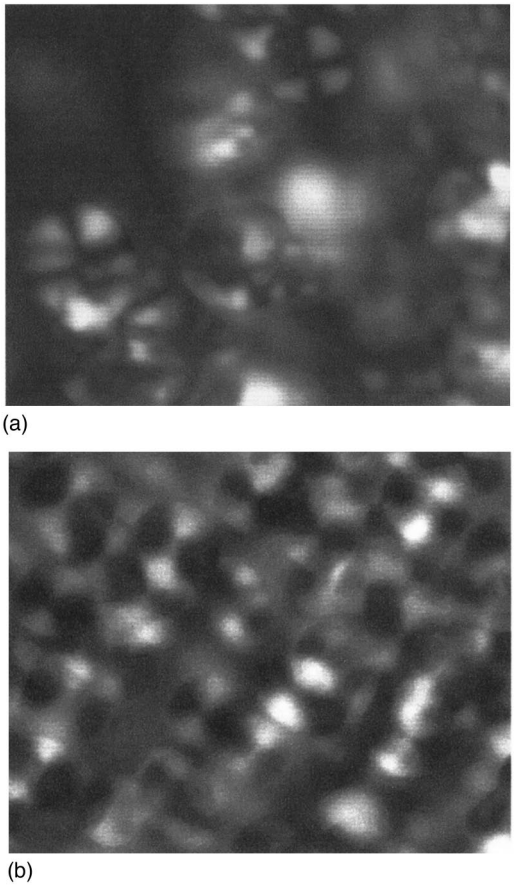

FIG. 2. Texture observed at rest under a polarizing microscope, (a) $\dot{\gamma}=200\,\mathrm{s}^{-1}$ and (b) $\dot{\gamma}=800\,\mathrm{s}^{-1}$.

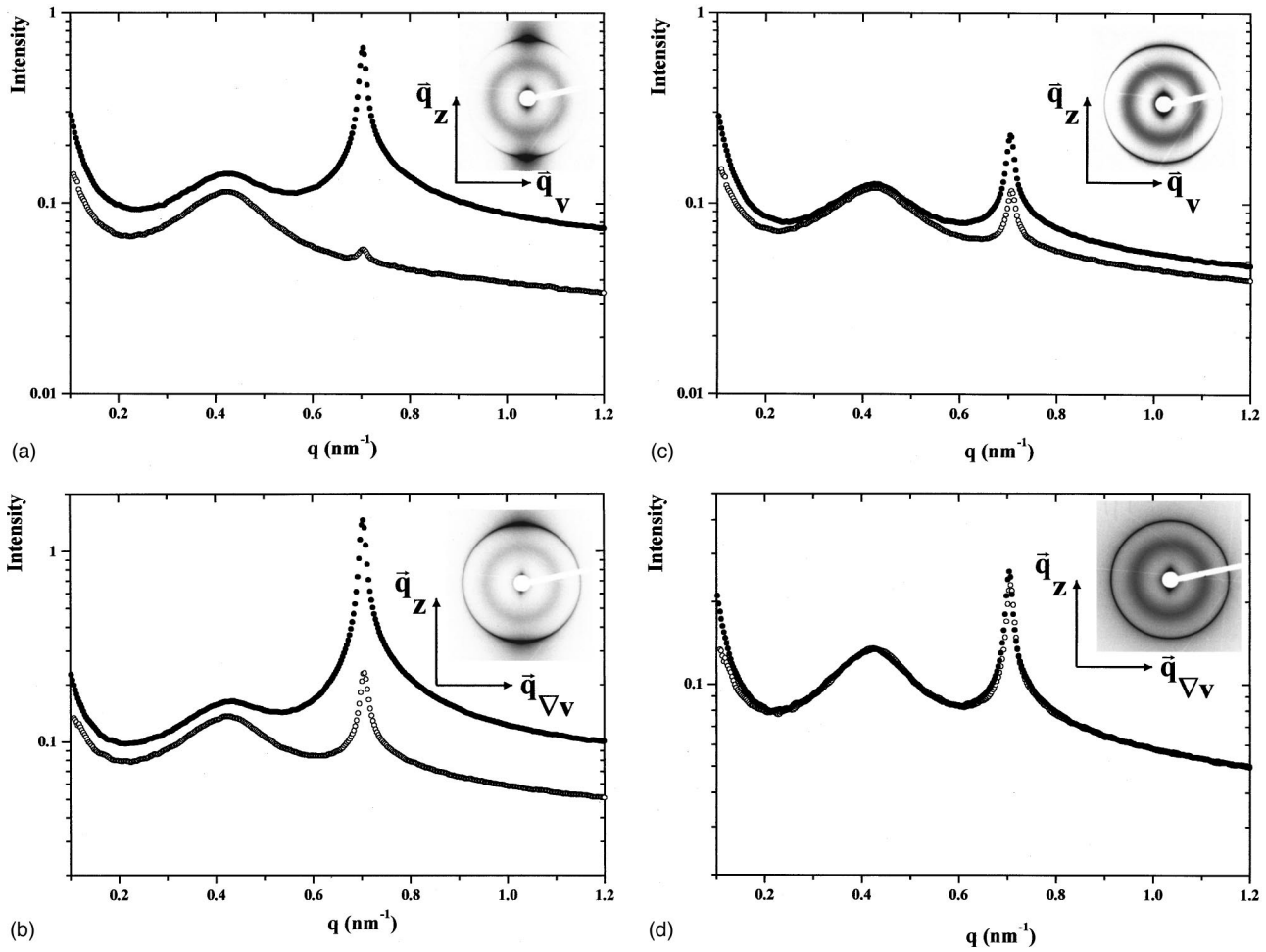

FIG. 3. SAXS profiles obtained in the different planes. The intensities are normalized to an absolute scale (per sterad mm). (a) Along the vorticity (closed circles) and the velocity (open circles) directions for $\dot{\gamma}=200\,\mathrm{s}^{-1}$. Inset: Two-dimensional (2D) pattern in the $(\vec{q}_v,\vec{q}_z)$ plane. (b) Along the vorticity (closed circles) and the shear gradient (open circles) directions for $\dot{\gamma}=200\,\mathrm{s}^{-1}$. Inset: 2D pattern in the $(\vec{q}_{\nabla v},\vec{q}_z)$ plane. (c) Along the vorticity (closed circles) and the velocity (open circles) directions for $\dot{\gamma}=800\,\mathrm{s}^{-1}$. Inset: 2D pattern in the $(\vec{q}_v,\vec{q}_z)$ plane. (d) Along the vorticity (closed circles) and the shear gradient (open circles) directions for $\dot{\gamma}=800\,\mathrm{s}^{-1}$. Inset: 2D pattern in the $(\vec{q}_{\nabla v},\vec{q}_z)$ plane.

depicted in Fig. 2(a). This indicates that the elongated domains under flow are made of the lamellar phase since the lamellar droplets observed at rest result from the Rayleigh instability. For $\dot{\gamma}\geqslant 480\,\mathrm{s}^{-1}$, the anisotropy vanishes and the scattering pattern becomes isotropic indicating that the elongated structures have been completely destroyed as can be seen in Fig. 1, inset c. The corresponding optical microscope picture [Fig. 2(b)] shows the presence of monodisperse multilamellar droplets immersed in the L_3-phase matrix that are slightly deformed [18].

The microstructure of these two steady states in the $(\vec{V},\vec{Z})$ and $(\nabla\vec{V},\vec{Z})$ planes can be probed by SAXS using a highly collimated beam that traverses through either the center of the cell (radial configuration) or the middle of the Couette gap (tangential configuration), respectively. Figures 3(a)–3(d) show typical scattering patterns obtained in the $(\vec{V},\vec{Z})$ and the $(\nabla\vec{V},\vec{Z})$ planes at low and high shear rates. SAXS data observed in the coexisting region of L_α/L_3 phases exhibit two peaks corresponding to a smectic distance $d=9.0\,\mathrm{nm}$ of the L_α phase and to the correlation length $\xi=14.9\,\mathrm{nm}$ of the L_3 phase. From the SAXS patterns observed in the radial and the tangential configurations, the orientation of each coexisting phase can be determined independently. The orientation of the L_3 phase is always isotropic under shear flow whereas the orientation of the L_α phase is strongly anisotropic at low shear rates but becomes more isotropic at high shear rates. In the anisotropic case, most of the membranes in the lamellar phase are oriented perpendicular to the vorticity direction. The proportion of the membranes of the L_α phase oriented in the $(\vec{V},\vec{Z})$ and $(\nabla\vec{V},\vec{Z})$ planes is determined by comparing the intensity of the corresponding Bragg peaks along the different directions, using the isotropic intensity of the L_3 phase as a reference. At low shear rates, we found that $I_z/I_v\approx 70$ and $I_z/I_{\nabla v}\approx 9$, where I_z, I_v, and $I_{\nabla v}$ are the intensity of the lamellar Bragg peak along $\vec{Z}$, $\vec{V}$, and $\nabla\vec{V}$, respectively. These results, when combined with the SALS data and optical microscopy, show that the anisotropy at $\dot{\gamma}\leqslant 370\,\mathrm{s}^{-1}$ corresponds to the existence of

elongated micron size domains along $\vec{V}$, which are composed of lamellar phase.

IV. DISCUSSION

Because of the interfacial tension between L_α and L_3 phases and the strong anisotropy observed in the $(\vec{V},\vec{Z})$ and $(\nabla\vec{V},\vec{Z})$ planes, the lamellar domains must be ribbonlike. Two different ribbonlike structures are consistent with our experimental data as discussed below.

(1) Multilamellar ribbonlike structures aligned in the flow direction and immersed in the L_3 phase. Recall that the strong anisotropy observed in the $(\nabla\vec{V},\vec{Z})$ plane shows that these elongated multilamellar objects cannot be cylinders, since the section of cylinders is isotropic in this plane, but instead ribbons. In a concentrated suspension like the samples studied here, scattering methods essentially provide the persistence length of these ribbonlike objects rather than their contour length or aspect ratio. In this study, SAXS probed only typical *q*-ranges corresponding to interlamellar distances. However, the intensity distribution of the SALS pattern reported in Fig. 1 (inset b) can be accurately fitted along the *Z* direction to a Lorentzian line shape. The width of the intensity profile is consistent with a ribbon persistence length of 10–15 μm. The ribbon dimensions can also be indirectly estimated from the texture observed under an optical microscope upon the cessation of flow, since the large lamellar droplets observed at rest [see Fig. 2(a)] result directly from the breakup of the ribbons via the Rayleigh instability. The size of the droplets (typically 20 μm) is intermediate between the length and the width of the ribbons. Very recently, Zipfel *et al.* [28] have reported the existence of elongated transient cylindrical multilamellar structures upon shearing a lamellar phase. However, these structures [28] differ from our findings, since that study pertains to the one-phase region and those transient structures breakup to form monodisperse multilamellar vesicles with continued shearing. In contrast to the small-angle neutron scattering (SANS) isotropic scattering patterns (for cylinders) observed by Zipfel *et al.* [28], in our case the scattering patterns at low shear rates in the tangential beam configuration exhibit a strong anisotropy [29] characteristic of the existence of ribbonlike structures.

*(2) Interlaced stacking of L_α and L_3 domains (shear bands) along **Z** direction*. This is similar to the *B*2 shear bands described by Olmsted [21]. Assuming their existence, SALS data show that these elongated domains along $\vec{V}$ must be ribbonlike since their dimension along $\vec{Z}$ should be typically 1 mm (the cell gap) [30]. Furthermore SALS shows that their geometry (horizontal in the Couette cell) remains identical whether the imposed variable is the stress or shear rate. This intriguing result drastically differs from shear banding [20–27] in complex fluids. When shear banding (i.e., coexistence between two steady states) is observed at a fixed shear rate, the transition between the two previous steady states becomes discontinuous if the stress is imposed [20–27]. In this situation one observes a hysteresis loop and a structural bistability: the shear bands are no longer present. Therefore the physics involved in our case is very different from that of shear banding. Indeed, if the domain stacking really exists, then it has not resulted from a shear induced coexistence between two different steady states (like in shear bands), but instead from a thermodynamic coexistence between two phases having different viscosities (L_α and L_3 phases in this case).

In summary, we have shown that in a L_α/L_3 phase-separated mixture at low shear rates, there exists a new steady state made of *multilamellar* ribbonlike structures. At high shear rates, these ribbons become unstable and fragment into monodisperse lamellar droplets. The existence of ribbonlike structures in the L_α/L_3 phase-separating mixture is very intriguing, since no similar structures have ever been reported in phase-separating binary fluids to the best of our knowledge.

ACKNOWLEDGMENTS

We thank J. P. Delville, F. Nallet, and K. Mortensen for helpful discussions. This work was supported by the Centre National de la Recherche Scientifique PICS (Grant No. 610) and by the Conseil Régional d'Aquitaine (CTP Grant No. 980209202). The European Synchrotron Radiation Facility is acknowledged for beam time allocation SC736.

[1] D. Myers, *Surfactant Science and Technology* (VCH, New York, 1992).
[2] P. Becher, *Emulsions: Theory and Practice* (Reinhold, New York, 1965).
[3] E. D. Siggia, Phys. Rev. A **20**, 595 (1979).
[4] A. Onuki, J. Phys.: Condens. Matter **9**, 6119 (1997).
[5] G. I. Taylor, Proc. R. Soc. London, Ser. A **146**, 501 (1934).
[6] D. Beysens, M. Gbadamassi, and L. Boyer, Phys. Rev. Lett. **43**, 1253 (1979).
[7] T. Baumberger, F. Perrot, and D. Beyssens, Physica A **174**, 31 (1991).
[8] K. Y. Min and W. I. Goldburg, Phys. Rev. Lett. **70**, 469 (1993).
[9] T. Hashimoto, K. Matsuzaka, and K. Fujioka, J. Chem. Phys. **108**, 6963 (1998).
[10] T. Hashimoto, K. Matsuzaka, E. Moses, and A. Onuki, Phys. Rev. Lett. **74**, 126 (1995); Phys. Rev. E **56**, 6970 (1997).
[11] A. Frischknecht, Phys. Rev. E **56**, 6970 (1997); **58**, 3495 (1998).
[12] P. Hervé, D. Roux, A. M. Bellocq, F. Nallet, and T. Gulik-Krzywicki, J. Phys. II **3**, 1255 (1993).
[13] G. Porte, J. Marignan, P. Bassereau, and R. May, J. Phys. (France) **49**, 511 (1988).
[14] D. Roux, F. Nallet, and O. Diat, Europhys. Lett. **24**, 53 (1993).
[15] O. Diat and D. Roux, J. Phys. II **3**, 9 (1993); O. Diat, D. Roux, and F. Nallet, *ibid.* **3**, 1427 (1993).
[16] H. F. Mahjoub, C. Bourgaux, P. Sergot, and M. Kleman, Phys. Rev. Lett. **81**, 2076 (1998).

[17] J. Yamamoto and H. Tanaka, Phys. Rev. Lett. **77**, 4390 (1996).
[18] G. Cristobal, J. Rouch, A. Colin, and P. Panizza, Phys. Rev. E **62**, 3871 (2000).
[19] M. Goveas and D. Pine, Europhys. Lett. **48**, 706 (1996).
[20] G. Porte, J. F. Berret, and J. L. Harden, J. Phys. II **7**, 459 (1997).
[21] P. Olmsted, Europhys. Lett. **48**, 339 (1999).
[22] M. E. Cates, T. C. B. McLeish, and G. Marucci, Europhys. Lett. **21**, 451 (1993).
[23] R. Malkhoufi, J. P. Decruppe, A. Ait-Ali, and R. Cressely, Europhys. Lett. **32**, 253 (1995).
[24] O. Diat, D. Roux, and F. Nallet, J. Phys. II **3**, 1427 (1993); Phys. Rev. E **51**, 3296 (1995).
[25] P. Panizza, P. Archambault, and D. Roux, J. Phys. II **5**, 303 (1995).
[26] D. Bonn, J. Meunier, O. Greffier, A. Al-Kahwaji, and H. Kellay, Phys. Rev. E **58**, 2115 (1998).
[27] M. M. Britton and P. T. Callaghan, Europhys. Lett. **36**, 719 (1996).
[28] J. Zipfel, F. Nettesheim, P. Lindner, T. D. Le, U. Olsson, and W. Richtering, Europhys. Lett. **53**, 335 (2001).
[29] Indeed, an asymmetry can be noticed in all SANS patterns obtained by Zipfel *et al.* in the tangential beam configuration (Fig. 2 of Ref. [22]). This extra intensity over a small azimuthal sector persists even in isotropic case (vesicles) and it directly results from a geometrical artifact because of the large neutron beam size compared to the 1 mm gap between the concentric cylinders. In the case of oriented lamellae, the intensity pattern along the $\vec{Z}$ direction should present two symmetrical peaks of same intensity.
[30] Note that if the dimension of the domains (or bands) along $\nabla\vec{V}$ differs from the gap of the cell, the influence of the surface tension between the two coexisting phases would likely tend to make multilamellar ribbonlike vesicles.